The Cryosphere Discuss., 6, 3079–3099, 2012
www.the-cryosphere-discuss.net/6/3079/2012/
doi:10.5194/tcd-6-3079-2012

The Cryosphere Discussions

Ground penetrating radar detection of subsnow liquid overflow on ice-covered lakes in interior Alaska

A. Gusmeroli[1] **and G. Grosse**[2]

[1]International Arctic Research Center, University of Alaska Fairbanks, Fairbanks, Alaska, USA
[2]Geophysical Institute, University of Alaska Fairbanks, Fairbanks, Alaska, USA

Received: 19 June 2012 – Accepted: 18 July 2012 – Published: 31 July 2012

Correspondence to: A. Gusmeroli (alessio@iarc.uaf.edu)

Published by Copernicus Publications on behalf of the European Geosciences Union.

Abstract

Lakes are abundant throughout the pan-Arctic region. For many of these lakes ice cover lasts for up to two thirds of the year. This frozen cover allows human access to these lakes, which are therefore used for many subsistence and recreational activities, including water harvesting, fishing, and skiing. Safe access to these lakes may be compromised, however, when, after significant snowfall, the weight of the snow acts on the ice and causes liquid water to spill through weak spots and overflow at the snow-ice interface. Since visual detection of subsnow liquid overflow (SLO) is almost impossible our understanding on SLO processes is still very limited and geophysical methods that allow SLO detection are desirable. In this study we demonstrate that a commercially available, lightweight 1 GHz, ground penetrating radar system can detect and map extent and intensity of SLO. Radar returns from wet snow-ice interfaces are at least twice as much in strength than returns from dry snow-ice interface. The presence of SLO also affects the quality of radar returns from the base of the lake ice. During dry conditions we were able to profile ice thickness of up to 1 m, conversely, we did not retrieve any ice-water returns in areas affected by SLO.

1 Introduction

Shallow lakes and ponds are abundant throughout the pan-Arctic region. These water bodies can have various origins, including thermokarst, glacial, fluvial, deltaic or structural (Smith et al., 2007; Jones et al., 2011; Arp and Jones, 2009). The surfaces of these lakes typically start to freeze in the fall and remain solid and ice covered until the spring. The freezing rate, ice growth, and resulting ice thickness are strongly conditioned by the amount of snow that resides above (Adams and Roulet, 1980; Liston and Hall, 1995; Sturm and Liston, 2003). Once formed, lake ice is also affected by cracking and fracturing due to thermal expansion and shrinkage during the lake ice formation, and wind-caused drift processes, often creating weak zones in the ice. Another process that adds weak zones in ice is strong year-round methane emission from lake and taberal sediments, causing inclusion of large gas bubbles in the vertical ice column and in some cases the maintaining of methane emission hotspots that remain open water throughout much of the year (Walter et al., 2006, 2010). During the winter, ice-covered freshwater lakes in the sub-Arctic have a tangible societal role. Lakes are visited for fishing, harvesting water, and recreational activities such as camping, skidoo travels, skiing and dog mushing.

Travel, work and recreation on frozen freshwater bodies present some hazards. The higher hazards are at the beginning and at the end of the ice-covered season when ice is either not yet thick and stable enough (fall) or begins to be structurally damaged from increasing temperature (spring). Another significant hazard present during the entire winter is the occurrence of severe overflow events (Fig. 1a). After a significant snowfall, the weight of the new snowpack acts on the ice and causes water to spill above the ice through weak spots, such as cracks or methane hot-spots. After an overflow event, the base of the snowpack changes from dry snow to water saturated snow (slush). In severe events (e.g. complete flooding of the snowpack, Fig. 1a) hazardous conditions are recognizable; in less severe, still hazardous cases (e.g. basal flooding, Figs. 1b and 1c), the direct visual detection of the presence of basal slush or liquid water beneath the snowpack is almost impossible, and the development of geophysical techniques for measuring snow and ice thickness and detecting subsnow water is desirable.

In this study, we employ a commercially available, portable, 1 GHz Ground Penetrating Radar (GPR) to study the radar characteristics of ice-covered lakes affected by liquid overflow in the snowpack. While the use of GPR to measure snow and lake-ice thickness is well known (Arcone et al., 1997), the detection of subsnow liquid overflow (SLO) using GPR has received little attention so far. We demonstrate that GPR is a powerful method to detect and map the presence and magnitude of SLO. This is because sub-snowpack water strongly affects the GPR signal. The GPR response to dry snow-ice interfaces was very different from the GPR response to wet snow-ice interface. During the dry case (no liquid overflow), the GPR signal was able to penetrate through the snow-ice interface and reflections from the base of the lake ice were successfully retrieved. Conversely, when the base of the snowpack was wet (extensive overflow), the signal was unable to penetrate to the base. Our findings indicate that it might be possible to develop routine mapping of SLO with ground-based and space-based radar.

2 Field area and methods

GPR measurements were made at 3 thermokarst lakes (Smith Lake, Ace Lake and Killarney Lake) in the Fairbanks area, interior Alaska. Surveys were made on 12 March (Smith Lake), 13 March (Ace Lake) and 21 March (Killarney Lake). The GPR system was a lightweight, commercially available PulseEkko Pro System with 1 GHz antennas connected to it. A handheld Garmin GPS system was attached to the GPR to store the coordinates of the GPR profiles. The survey was operated in standard GPR reflection mode. The GPR system emits radar pulses which are reflected by the interface between the snow and the top of the lake ice. The second event recorded in these surveys is the reflection from the base of the lake ice. The travel time of this reflection from the ground can be used to estimate snow and ice depth.

GPR is a powerful tool for non-destructively measuring snow and ice thickness in cold regions. Many authors have used GPR (or FM-CW radar) to characterize Alpine (Marshall et al., 2005; Bradford et al., 2009b; Heilig et al., 2010), Arctic (Holmgren et al., 1998), and on-glacier (Macguth et al., 2006) snowpack. Studies on freshwater ice have demonstrated that GPR can profile lake ice (Arcone et al., 1997) and river ice (Arcone and Delaney, 1987) thickness. The clarity, the spatial continuity and the very shallow position of shallow cryospheric targets typically results in reliable GPR depth estimates with minimal signal processing (e.g. Macguth et al., 2006; Gusmeroli et al., 2012). The only processing applied to the data was the removal of the instrumental, low-frequency noise that is typical of GPR systems. This low frequency noise is known as “wow” in the radar literature, and the filter associated to it is called dewow.

TCD
6, 3079–3099, 2012

A. Gusmeroli and G. Grosse

In addition to GPR data, we collected data of snow thickness, slush thickness, ice thickness, and total water depth in several locations along the GPR profiles.

3 Results

On all three lakes snow thickness ranged from 30–70 cm, ice thickness was 49–65 cm, and water depth from 0 to 695 cm. A substantial late-season snowfall (20–40 cm of new snow in two days) in the week before our surveys in early March 2012 strongly increased snow weight on the ice, causing overflows in various areas of many lakes. Slush thickness at Ace and Killarney Lake ranged 2–22 cm and was highly variable within a lake area and between lakes. Figure 1c shows details of the snowpack at Ace Lake in case of SLO.

We identified two different GPR-snow-ice characteristics that were distintinctly different between dry-based snowpack and wet-based snowpack.

3.1 Dry snow-ice interface, no overflow.

At Smith Lake (Fig. 2a), there was no sign of water at the base of the snowpack. The snow-ice interface was dry. The GPR profiles were purposely collected on thee different types of snowpacks: (i) a well-compacted snowpack on an established ski trail (Profile AB, Fig. 2b); (ii) a disturbed snowpack, in which a trail was established prior to GPR survey (BC, Fig. 2c); and (iii) a pristine snowpack in which the GPR was allowed to float on the fresh snow surface (Profile CA, Fig. 2c). Results in Fig. 2 are presented with GPR two-way travel times. Thickness bars, included for comparison, were derived by assuming radar wave speeds of 0.21, 0.25 and 0.168 $\mathrm{m\,ns^{-1}}$ for compacted snow, loose snow, and ice, respectively (Robin, 1975). These velocities are typically observed in snow-ice studies and are consistent with measurements obtained in the field.

From all three GPR profiles collected at Smith Lake we can distinguish two prominent reflectors (Fig. 2). The shallower reflector is the snow-ice interface. The deeper reflector is the ice-water or the ice-sediment interface. Results are very sensitive to the conditions of the snowpack. The clearest reflections are observable in the compacted snowpack (Fig. 2a) and in the pristine snowpack (Fig. 2c). The clarity and the spatial continuity of the reflectors is less appreciable on the newly established snow trail, most likely because the GPR is towed over an irregular surface. The internal ice reflectors observable in Fig. 2b and c are caused by survey cables lying on the snow (we conducted our GPR surveys at the same time with other geophysical investigations). To summarize, this 1 GHz GPR survey in a dry snow-ice interface situation successfully retrieved reflections from the base of the lake ice.

3.2 Wet snow-ice interface, overflow present.

At Ace and Killarney Lakes, we noticed that liquid water was present beneath the snowpack (e.g. Fig. 1b at Ace Lake). Both thermokarst lakes had a substantial number of methane emission hotspots of 10–30 cm in diameter that were only covered with a thin crust of ice and snow only, while the other areas of both lakes were covered with ice ranging in thickness from 49–65 cm. The overflow water was in the form of basal slush on 12–13 March and started to freeze subsequently. Granular snow-ice (flooded snow with refrozen liquid phase) with some degree of wetness was observed in the following days until late March. As the temperatures rose above freezing, snowmelt started, and it became impossible to distinguish whether the basal snow wetness was due to SLO or water percolation from surface melt. In any case a persistently wet snow-ice interface was observed from 12 March until the beginning of the snowmelt. Once the snowmelt started at the end of March, it was not possible to discern whether basal snow-wetness was due to snow melt or SLO.

At Ace Lake we undertook a variety of GPR profiles, including a line crossing the entire lake (Fig. 3a) and a detailed study on the shores (Fig. 3b). The long profile showed a surprising behavior: the reflections from the base of the lake ice were only detectable nearby the shore. Over the vast majority of the lake, the ice-water reflections were obscured by a high amplitude series of echoes from the wet snow-ice interface (Fig. 3c).

The detailed study on the shore revealed other interesting features of SLO (Fig. 3b). The strength of the snow-ice echoes gradually increased when moving from dry snow-ice conditions into wet snow-ice conditions (Fig. 3d–f). The strength of the ice-water echoes behaved oppositely. The snow depth on the shore of the lake was about twice the snow depth on the lake (Fig. 3e, f).

Similar results were noticed at Killarney Lake (Fig. 4a). The Killarney case study provides an excellent example for spatial variability of SLO. At Killarney (Fig. 4), we noticed spatial variability in the intensity of the snow-ice reflection (e.g. 30–40 in Fig. 4b; 20–30 m in Fig. 4c; and the general pattern in Fig. 4d). This is particularly clear when the reflection is studied in detail (Fig. 5). By using the spectral amplitude, we can quantify the intensity of the reflection (Fig. 5a for the radargram and 5b for the intensity). The spectral amplitude was three times higher in regions affected by severe overflow: the magnitude of subsnow overflow events can therefore be quantified using high frequency GPR.

4 Discussion

4.1 Slush water content

Spatial variability in basal-snow reflectivity (e.g. Fig. 5) suggest that on-lake SLO distribution is heterogeneous (e.g. with different values of slush water content). We now undertake a simple modeling exercise to further understand this. Specifically we aim to provide a first order estimate of the volumetric fraction of water within the basal snow (w). We do this by generating a synthetic GPR dataset. The response of the model will then be compared to our data to provide a quantification of w. Our modeling exercise is very similar to the one applied recently by Bradford et al. (2009a); in their study Bradford et al. (2009a) generate synthetic GPR data in order to assess the usefulness

TCD
6, 3079–3099, 2012

of basal-snow reflectivity to detect oil under snow on the sea ice. They noticed that 2-cm-thick oil film trapped between snow and sea ice could be detected based on a 51% decrease in reflection strength.

We simulated the GPR response using the free-source modeling package MATGPR (http://users.uoa.gr/~atzanis/matgpr/matgpr.html). The model is based on the FDTD (finite difference time domain) treatment of Maxwell's equations (Irving and Knight, 2006; Tzanis, 2006) and only requires model-geometry (Fig. 6a) and dielectric permittivity (ε Table 1) as input. We simulate a GPR survey over different regions: one with dry snow-ice interface (Fig. 6a, b, b1); one with a 18 cm layer of slush with water content $w = 30\%$ between snow and ice (Fig. 6a, b, b2) and one with a 18 cm layer of slush with $w = 10\%$ between snow and ice (Fig. 6a, b, b3). The effect that water content has on dielectric permittivities was simulated by considering slush as a 2 phase dielectric medium composed by snow and water (Table 1).

Figure 6 shows the results of the simulation. As noticed from the field data, the amplitude of the reflections from the base of the snowpack changes according to the properties of the basal material. Amplitude is lowest for a dry snow-ice interface (Fig. 6 blue arrow, wavelet b1) dramatically increases of ~ 6 times with basal slush $w = 30\%$ (Fig. 6 red arrow, wavelet b2) and of ~ 4 times with basal slush $w = 10\%$ (Fig. 6 green arrow, wavelet b3). The behavior of the modeled ice-water reflection is also consistent with what we have observed in the field data (Fig. 6). Ice-water returns are stronger in the case of no overflow. The presence of overflow changes the dielectric properties of snow, greatly attenuates the radar energy and degenerate the quality of the ice-water returns (Fig. 6). From our simple modeling we can argue that slush $w > 10\%$ is necessary for obscuring the the ice-water reflection.

4.2 Radar characteristics of ice covered lakes

Arcone et al. (1997) studied lakes on the Alaskan North Slope and demonstrated that X and C band FM-CW radar can be used to profile lake ice thickness. They also showed that the intensity of the reflection from the base of the lake ice was much higher for floating ice than it was in grounded ice. This observation is noticeable also in our radar profiles. One profile at Smith Lake (Fig. 2b) shows very high ice thickness (1.3 m) and weaker returns than the other two profiles (Fig. 2c, d). Smith Lake was indeed the shallowest lake of our study and the lake ice was grounded. Observations from boreholes penetrating the lake ice indicate that some liquid water was present at the base of the ice in some locations, suggesting that the sediment has not been freezing at these sites, while at other sites no water was encountered. The differences in radar intensity in the profiles at Smith Lake can be explained by considering alternating frozen to the bottom (dry ice-soil interface, weak return – Fig. 2b) and wet based (water at the base, strong return – Fig. 2c, d) lake ice conditions. The study of Arcone et al. (1997) was undertaken with dry snow-ice conditions. In dry conditions, it is possible to continuously profile lake-ice (Arcone et al., 1997); in wet conditions, instead, the presence of liquid water beneath the snowpack strongly affects the radar response. The intensity of the GPR reflection is much higher in the case of a wet snow-ice interface. The occurrence of radar returns from the base of the lake ice strongly depends on the presence or absence of SLO. The presence of SLO impedes penetration of the radar signal into the lake ice. This is because SLO moisturizes the snowpack and increases its dielectric permittivity (Fig. 6).

From our GPR profiles we can also notice the potent insulating effect of the snow cover. In some locations our GPR surveys intersected established ski paths (e.g. Fig. 2b and arrows in Fig. 5). Snow on substantially compacted, established ski-paths is very different than pristine snow: it is thinner, denser and has a much higher thermal conductivity than the pristine sub arctic snow composed prevalently by coarse, low-density, depth hoar layers (Sturm and Johnson, 1992; Sturm et al., 1997; Zhang, 1996). In a pristine sub-Arctic snow pack the depth hoar fraction can be over 50 % (Sturm and Johnson, 1992). The effective thermal conductivity of the depth-hoar is 0.063 W m^{-1} K^{-1}, about one fifth to one twentieth the value of high density packed slabs. It is therefore likely that the thicker ice, frozen to the bottom in Fig. 2b is due to the smaller insulating effect of the packed snow cover. At Killarney Lake the presence of moderately compacted ski-trails, freshly established on the day before our GPR survey, caused water overflow to freeze overnight. These areas are noticeable in the GPR data by the sporadic appearing of the ice-water reflector when the GPR profile intersected the ski trails (white arrows in Fig. 5).

Our results have implications on the use of Synthetic Aperture Radar (SAR) imagery for the study of Arctic lakes. SAR techniques are known to be an effective way to characterize Arctic lake ice (Jeffries et al., 1998). Space-borne SAR studies investigating seasonal lake ice characteristics in high latitude lakes indicate that snow characteristics may be an important factor for radar backscatter during different parts of the season. For example, Duguay et al. (2002) suggest that an observed decrease in Radarsat-1 backscatter for sub-Arctic lake ice during spring is related to lake ice decay, ponding on the lake ice surfaces, and also wet snow. The presence of basal slush and snow-ice (granular ice formed by refreezing SLO) is commonly reported in SAR and lake-ice studies (Adams and Roulet, 1980; Duguay et al., 2003; Nolan et al., 2003; Walter et al., 2008). Nolan et al. (2003) suggested that snow-ice formation is an occasional, localized phenomenon detectable as cracks from SAR imagery of a large Siberian lake. In both Ace Lake and Killarney Lake, the GPR profile shows that basal-slush (and subsequent snow-ice formation) is widespread on the lake. Walter et al. (2008) recognized the potential confounding role of slush in SAR studies of methane bubbles trapped in lake ice and suggested that SAR studies focused on methane ebullition might perform best in early winter, before SLO and snow-ice generating large snowfalls. Our results show that presence or absence of SLO is a primary control on the radar returns from the snow-ice and ice-water interfaces. Future work should focus on quantitative studies of SLO as well as assessment of spatial and temporal distribution of SLO.

4.3 Changing lakes in a changing climate

Several studies indicate that Arctic lakes are important components of the climate system (Brown et al., 2010; Latifovic and Pouliot, 2007) and are changing rapidly with current climate shifts in northern high latitudes. Climate warming will have a profound

TCD
6, 3079–3099, 2012

impact on the thermal characteristics of lakes, ice, and snow cover (Arp et al., 2010). Observations from the Arctic Coastal Plain indicate that lake ice regimes are shifting from grounded ice towards floating ice lakes due to thinner ice cover (Arp et al., 2011). Thinning of ice cover in Subarctic and Arctic lakes, in combination with a projected increase of winter precipitation for many regions (Arctic Monitoring Assessment Programme, 2011) may increase the occurrence of SLO. In this evolving situation GPR will be a useful tool to monitor lake ice dynamics, spatially and temporally.

5 Conclusions

Ice-covered shallow lakes and ponds are ubiquitous during the winter in the Arctic. Northern communities use these lakes for recreation and subsistence. Safe access to the lakes is guaranteed when the ice is thick enough and there is no liquid water beneath the snowpack. Radar systems such as Ground Penetrating Radar and FM-CW Radar are typically used to measure ice thickness, but no method has yet been proposed to detect and spatially characterize the presence of subsnow liquid overflow (SLO). In this study we have shown that a lightweight, user-friendly, commercially available 1 GHz Ground Penetrating Radar system is able to detect presence and magnitude of SLO. The presence of SLO was a significant problem in profiling ice thickness. When SLO was present, no reflection from the ice base was retrievable. Our results suggest that future GPR surveys devoted to ice thickness measurements of Northern Lakes should not be conducted while SLO is on the ice (e.g. just after a significant snowfall). A similar GPR, mounted on remotely controlled, unmanned small aircrafts can provide a safe way to detect extent and magnitude of SLO over frozen freshwater bodies.

Acknowledgements. The project described in this publication was supported by the Alaska Climate Science Center, funded by Cooperative Agreement Number G10AC00588 from the United States Geological Survey. Its contents are solely the responsibility of the authors and do not necessarily represent the official views of USGS. GG was supported by NASA grant

TCD
6, 3079–3099, 2012

NNX08AJ37G and NSF ARC-1107607. We thank S. Fowell, E.C. Pettit and C. Wyatt of the Department of Geology and Geophysics at the University of Alaska Fairbanks for their availability letting us borrow their GPR system. A. Parsekian provided an informal review which improved the manuscript. C. Arp is also acknowledged for valuable help in the field. AG thanks L. Hinzman, S. Rupp, J. Walsh, M. Sturm and S. Filhol for support, encouragement and inspirational discussions about snow and ice. N. Bauer provided useful edits.

References

Adams, W. P. and Roulet, N. T.: Illustration of the roles of snow in the evolution of the winter cover of a lake, Arctic, 33, 100–116, 1980. 3080, 3088

AMAP, 2011: Snow, Water, Ice and Permafrost in the Arctic (SWIPA): Climate Change and the Cryosphere, Arctic Monitoring and Assessment Programme (AMAP), Oslo, Norway, xii + 538 pp., 2011. 3089

Arcone, S. A. and Delaney, A. J.: Airborne river-ice thickness profiling with helicopter-borne UHF short-pulse radar, J. Glaciol., 33, 330–340, 1987. 3082

Arcone S. A., Yankelun, N. E., and Chacho, E. F.: Reflection profiling of Arctic lake ice using microwave FM-CW radar, IEEE Trans. Remote S., 35, 436–443. 1997. 3081, 3082, 3086, 3087

Arp, C. D. and Jones, B. M.: Geography of Alaska lake districts: identification, description, and analysis of lake-rich regions of a diverse and dynamic state, US Geol. Surv. Sci. Invest. Rep., 2008-5215, 2009. 3080

Arp, C., Jones, B., Whitman, M., Larsen, A., and Urban, F.: Lake temperature and ice cover regimes in the Alaskan Subarctic and Arctic: integrated monitoring, remote sensing, and modeling, JAWRA J. Am. Water Resourc. Assoc., 46, 777–791, 2010. 3089

Arp, C. D., Jones, B. M., Urban, F. E., and Grosse, G.: Hydrogeomorphic processes of thermokarst lakes with grounded-ice and floating-ice regimes on the Arctic coastal plain, Alaska, Hydrol. Process., 25, 2422–2438, doi:10.1002/hyp.8019, 2011. 3089

Bradford, J. H., Dickins, D. F., and Brandvik, P. J.: Assessing the potential to detect oil spills in and under snow using airborne ground-penetrating radar, Geophysics, 75, G1–G12, 2009a. 3085

Bradford, J. H., Harper, J. T., and Brown, J.: Complex dielectric permittivity measurements from ground-penetrating radar data to estimate snow liquid water content in the pendular regime, Water Resour. Res., 45, W08403, doi:10.1029/2008WR007341, 2009b. 3082

Brown, L. C. and Duguay, C. R.: The response and role of ice cover in lake-climate interactions, Progress Phys. Geogr., 34, 671–704, 2010. 3088

Duguay, C. R., Pultz, T. J., Lafleur, P. M., and Drai, D.: RADARSAT backscatter characteristics of ice growing on shallow sub-Arctic lakes, Churchill, Manitoba, Canada, Hydrol. Process., 16, 1631–1644, 2002. 3088

Duguay, C. R. and Lafleur, P. M.: Determining depth and ice thickness of shallow sub-Arctic lakes using space-borne optical and SAR data, Int. J. Remote Sens., 24, 475–489, 2003. 3088

Gusmeroli, A., Jansson, P., Pettersson, R., and Murray, T.: Twenty years of cold surface layer thinning at Storglaciären, sub-Arctic Sweden, 1989–2009, J. Glaciol., 58, 3–10, doi:10.3189/2012JoG11J018, 2012. 3082

Heilig, A., Eisen, O., and Schneebeli, M.: Temporal observations of a seasonal snowpack using upward-looking GPR, Hydrol. Process., 24, 3133–3145, doi:10.1002/hyp.7749, 2010. 3082

Holmgren J., Sturm, M., Yankeluin, N. E., and Koh, G.: Extensive measurements of snow depth using FM-CW radar, Cold Regions Sci. Technol., 27, 17–30, 1998. 3082

Irving, J. and Knight, R.: Numerical modeling of ground-penetrating radar in 2-D using MATLAB, Comput. Geosci., 32, 1247–1258, 2006. 3086

Jeffries, M. O., Zhang, T., Frey, K., and Kozlenko, N.: Estimating late-winter heat flow to the atmosphere from the lake-dominated Alaskan North Slope, J. Glaciol., 45, 315–324, 1998. 3088

Jones, B. M., Grosse, G., Arp, C. D., Jones, M. C., Walter Anthony, K. M., and Romanovsky, V. E.: Modern thermokarst lake dynamics in the continuous permafrost zone, Northern Seward Peninsula, Alaska, J. Geophys. Res., 116, G00M03, doi:10.1029/2011JG001666, 2011. 3080

Latifovic, R. and Pouliot, D.: Analysis of climate change impacts on lake ice phenology in Canada using the historical satellite data record, Remote Sens. Environ., 106, 492–507, 2007. 3088

Liston, G. E. and Hall, D. K.: An energy-balance model of lake-ice evolution, J. Glaciol., 41, 373–382, 1995. 3080

TCD
6, 3079–3099, 2012

GPR detection of subsnow water on boreal lakes

A. Gusmeroli and G. Grosse

Title Page
Abstract | Introduction
Conclusions | References
Tables | Figures
◄| |►
◄ ►
Back | Close
Full Screen / Esc
Printer-friendly Version
Interactive Discussion

Macguth, H., Eisen, O., Paul, F., and Hoelzle, M.: Strong spatial variability of snow accumulation observed with helicopter-borne GPR on two adjacent Alpine glaciers, Geophys. Res. Lett., 33, L13503, doi:10.1029/2006GL026576, 2006. 3082

Marshall, H. P., Koh, G., and Forster, R. R.: Estimating Alpine snowpack properties using FMCW radar, Ann. Glaciol., 40, 157–162, 2005. 3082

Nolan, M., Liston, G., Prokein, P., Brigham-Grette, J., Sharpton, V. L., and Huntzinger, R.: Analysis of lake ice dynamics and morphology on Lake El'gygytgyn, NE Siberia, using synthetic aperture radar (SAR) and Landsat, J. Geophys. Res., 107, 8162, doi:10.1029/2001JD000934 , 2003. 3088

Smith, L. C., Sheng, Y., and MacDonald, G. M.: A first pan-Arctic assessment of the influence of glaciation, permafrost, topography and peatlands on Northern Hemisphere lake distribution, Permafrost Periglac., 18, 201–208, doi:10.1002/ppp.581, 2007. 3080

Sturm, M. and Johnson, J.: Thermal conductivity measurements of depth hoar, J. Geophys. Res., 97, 2129–2139, 1992. 3087

Sturm, M., Holmgren, J., Konig, M., and Morris, K.: The thermal conductivity of seasonal snow, J. Glaciol., 43, 26–41, 1997. 3087

Sturm, M. and Liston, G.: The snow cover on lakes of the Arctic coastal plain of Alaska, USA J. Glaciol., 49, 370–380, 2003. 3080

Walter, K. M., Zimov, S. A., Chanton, J. P., Verbyla, D., and Chapin III, F. S.: Methane bubbling from Siberian thaw lakes as a positive feed-back to climate warming, Nature, 443, 71–75, doi:10.1038/nature05040, 2006. 3081

Walter, K. M., Engram, M., Duguay, C. R., Jeffries, M. O., and Chapin, F. S.: The potential use of synthetic aperture radar for estimating methane ebullition from Arctic lakes, J. Am. Water Resourc. Ass., 44, 305–315, 2008. 3088

Walter Anthony, K. M., Vas, D., Brosius, L., Chapin III, F. S., Zimov, S. A., and Zhuang, Q.: Estimating methane emissions from northern lakes using ice bubble surveys, Limnol. Oceanogr. Methods, 8, 592–609, 2010. 3081

Robin, G.: Velocity of radio waves in ice by means of a bore-hole interferometric technique, J. Glaciol., 15, 151–158, 1975. 3083

Tzanis, A.: MATGPR: a freeware MATLAB package for the analysis of common-offset GPR data, Geophys. Res. Abstr., 8, 09488, EGU06-A-09488, 2006. 3086

Zhang, T., Osterkamp, T. E. and Stamnes, K.: Influence of the depth hoard layer of the seasonal snow cover on the ground thermal regime, Water Resour. Res., 32, 2075–2086, 1996. 3087

Table 1. Parameters used in the synthetic model.

Medium	ε
Water	80
Ice	3.2
Dry snow	1.68
Slush w = 30 %	25.12
Slush w = 10 %	9.44

TCD
6, 3079–3099, 2012

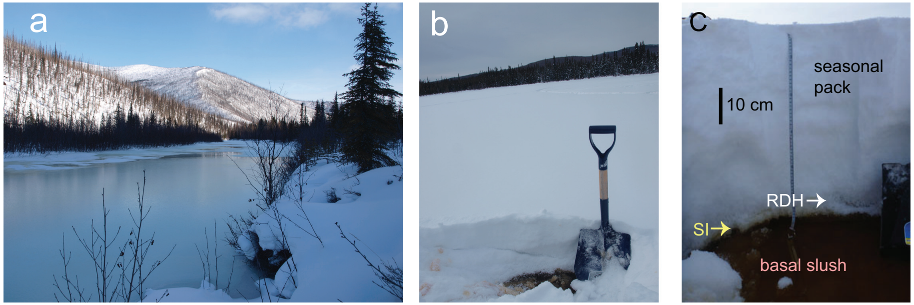

Fig. 1. (a) one of the most severe overflow event we have noticed in the winter 2012 on freshwater bodies in the vicinity of Fairbanks. The photo shows the West Fork of the Chena River on 11 March 2012. Safe access to the river is impeded by a vast amount of water which entirely flooded the snowpack. The photo pictures an area in which overflow is clearly visible to human eye. In some areas (also visible in the picture) overflow water did not flood the snowpack as a whole; in this case the hazard is still high but is not as visible. The cross section of the river is approximately 20 m. **(b)** the overflow event at Ace Lake on 15 March 2012. Liquid water only flooded the basal part of the snowpack. A detail of the wet snow base is provided in **(c)**. Rounded depth hoar (RDH) and snow-ice (SI) above the slush are visible.

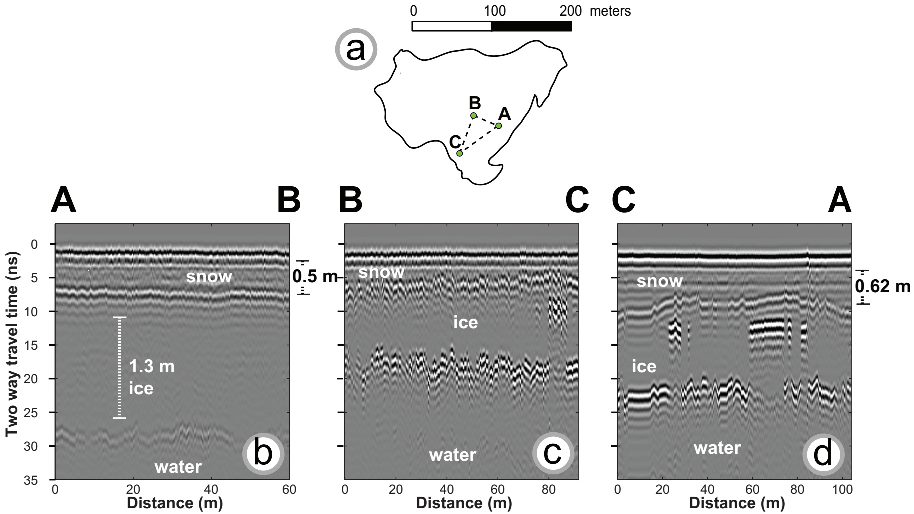

Fig. 2. 1 GHz GPR profiles acquired at Smith Lake. No overflow water was noticed at the snow-ice interface. Bars indicating thicknesses in snow and ice were calculated using radar speed in snow of $0.21\,\mathrm{m\,ns^{-1}}$ (**b**; compacted snow); $0.25\,\mathrm{m\,ns^{-1}}$ (**c**, **d**; loose snow) and $0.168\,\mathrm{m\,ns^{-1}}$ in ice.

TCD
6, 3079–3099, 2012

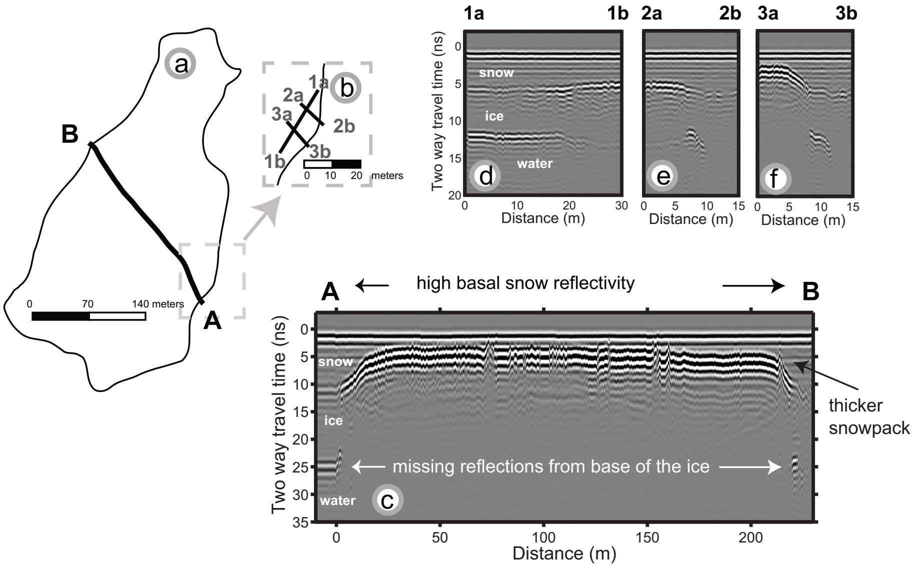

Fig. 3. 1 GHz GPR profiles acquired at Ace Lake. Extensive overflow water was noticed at the snow-ice interface. **(b)** shows a detailed study on the margin of the lake. **(c)** is the profile across the lake; **(d, e, f)** are detailed profiles (see **b** for location).

TCD
6, 3079–3099, 2012

GPR detection of subsnow water on boreal lakes

A. Gusmeroli and G. Grosse

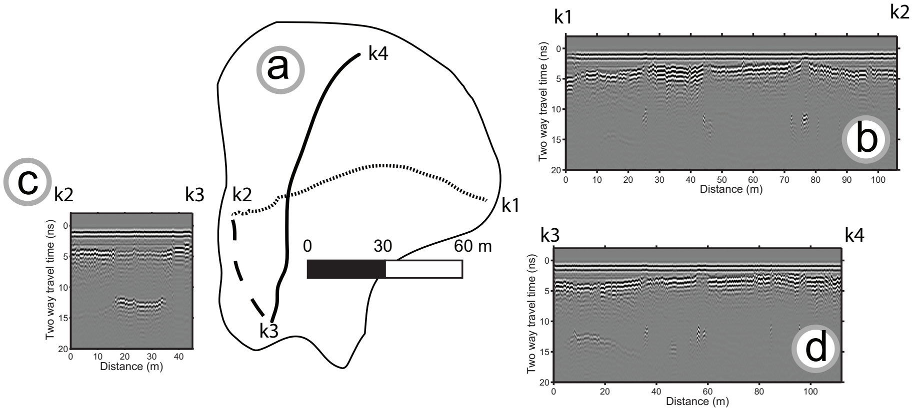

Fig. 4. 1 GHz GPR profiles acquired at Killarney Lake. Variable overflow water was noticed at the snow-ice interface. That the intensity of the snow-ice reflection is variable.

TCD
6, 3079–3099, 2012

GPR detection of subsnow water on boreal lakes

A. Gusmeroli and G. Grosse

Title Page
Abstract | Introduction
Conclusions | References
Tables | Figures
◀| |▶
◀ ▶
Back | Close
Full Screen / Esc
Printer-friendly Version
Interactive Discussion

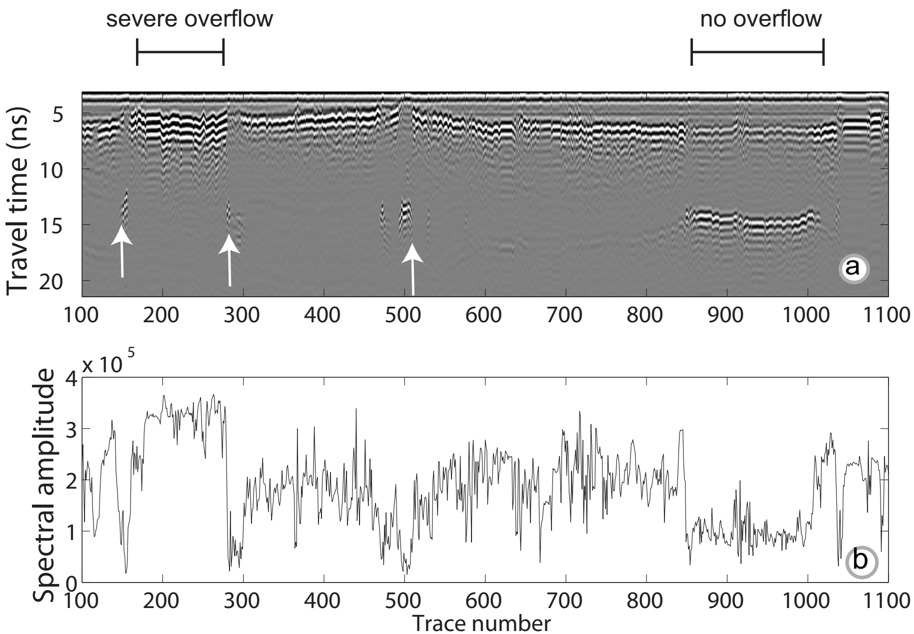

Fig. 5. Detailed analysis of the snow-ice reflections at Killarney lake. **(a)** shows the GPR data acquired all over the lake whereas **(b)** shows the intensity of the reflection measured using the peak amplitude of the Fast Fourier Transform. The magnitude of the intensity varies with space and is controlled by the presence of overflow water. White arrows indicate points in which the GPR profile crossed ski paths (see discussion in text).

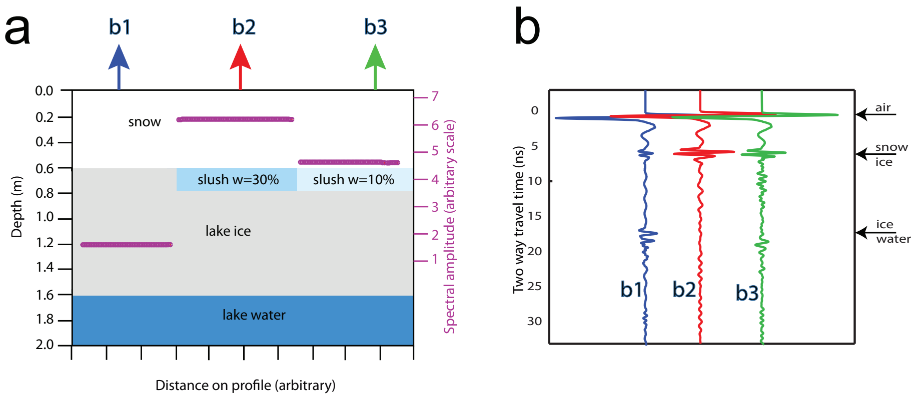

Fig. 6. Synthetic model of a GPR survey over lake ice. **(a)** Model configuration and simulated spectral amplitude (purple lines and purple scale on left) of the snow-base reflection. Returns from slush with water content $w = 30\,\%$ are nearly 6 times stronger than returns from a dry snow ice interface. The detail on the modeled GPR wavelets is depicted in **(b)**. Clear returns from lake ice-lake water are observable for the dry case (b1). Increasing of slush decreases the strength of the ice-water returns (b2, b3).